Chem. Mater. **2000,** *12,* 1367−1371

Electrochemical In-Situ Conductivity Measurements for Thin Film of $Li_{1-x}Mn_2O_4$ Spinel

Matsuhiko Nishizawa, Tomoaki Ise, Hiromichi Koshika, Takashi Itoh, and Isamu Uchida*

Department of Applied Chemistry, Graduate School of Engineering, Tohoku University, Aramaki-Aoba 07, Aoba-Ku, Sendai 980-8579, Japan

Received November 2, 1999. Revised Manuscript Received February 8, 2000

Electrical conductivity of $LiMn_2O_4$, which is a promising cathode active material for lithium ion batteries, was monitored in situ during electrochemical lithium extraction and reinsertion reactions in 1 M $LiClO_4$ propylene carbonate solution. The in-situ conductivity measurement was achieved by means of an interdigitated microarray electrode coated with a uniform and dense film of $LiMn_2O_4$. The conductivity of $Li_{1-x}Mn_2O_4$ was found to exhibit a peak-shaped profile as a function of lithium content. The conductivity of Cr^{3+}-doped spinel, $LiMn_{1.95}Cr_{0.05}O_4$, decreased monotonically with decreasing lithium content. These results are discussed by considering the effects of phase transformation on the conductivity of these materials.

Introduction

Lithium ion batteries consisting of lithium insertion materials, such as spinel $LiMn_2O_4$, are the state-of-the-art rechargeable power sources for consumer electronics.[1−9] Among the characteristics of insertion materials, the electrical conductivity of the component materials is one of the most important issues in connection with the rate performance of batteries. In addition to such practical importance, conductivity measurements during the lithium insertion (and extraction) reaction would be an attractive approach to study the variation in the electronic structure of the materials as a function of lithium content. Work in our laboratory has shown that the interdigitated microarray electrode (IDA electrode) is a powerful tool to study the dynamic changes in dc conductivity of electroactive materials such as conducting polymers and fullerenes.[10] We have recently applied this technique to research regarding lithium ion batteries.[11] For example, we observed the insulator−metal transition of $Li_{1-x}CoO_2$, for the first time experimentally.[12] The conductivity of a single particle of mesocarbon microbead (MCMB) was also measured and discussed in connection with the lithium insertion mechanism.[13]

In the present work, we study spinel $LiMn_2O_4$ which is an attractive cathode material for lithium ion batteries owing to its cost and environmental performance.[1−9] We employed the electrostatic spray deposition (ESD) method to prepare a thin film of spinel $LiMn_2O_4$ on the IDA electrode substrates.[14,15] A main result of this work is an unexpected transient increase in the conductivity during the course of lithium extraction (and reinsertion). We will attempt to explain this behavior by taking account of the two-phase reaction[6,9] characteristic of $Li_{1-x}Mn_2O_4$. We also studied ESD films of manganese-substituted spinels, $LiMn_{2-y}M_yO_4$ (M: Co or Cr), which have attracted much attention to improve cycling behavior of manganese oxide spinels.[16−18]

Experimental Section

The interdigitated array (IDA) electrode was fabricated by photolithography with a sputter-deposited Pt film on a ther-

---

* Corresponding author. E-mail: uchida@est.che.tohoku.ac.jp. Fax: +81-22-214-8646.

(1) Bruce, P. G. *Chem. Commun.* **1997**, 1817.

(2) Thackeray, M. M.; David, W. I. F.; Bruce, P. G.; Goodenough, J. B. *Mater. Res. Bull.* **1983**, *18*, 461.

(3) Tarascon, J. M.; Guyomard, D. *Electrochim. Acta* **1993**, *38*, 1221.

(4) Gao, Y.; Reimers, J. N.; Dahn, J. R. *Phys. Rev. B* **1996**, *54*, 3878.

(5) Gao, Y.; Dahn, J. R. *J. Electrochem. Soc.* **1996**, *143*, 100.

(6) Ohzuku, T.; Kitagawa, M.; Hirai, T. *J. Electrochem. Soc.* **1990**, *137*, 769.

(7) *Lithium Batteries, New Materials, Developments and Perspectives*; Pistoia, G., Ed.; Elsevier: Amsterdam, 1994.

(8) Pistoia, G.; Zane, D.; Zhang, Y. *J. Electrochem. Soc.* **1995**, *142* 2551.

(9) Liu, W.; Kowal, K.; Farrington, G. C. *J. Electrochem. Soc.* **1998**, *145*, 459.

(10) (a) Nishizawa, M.; Shibuya, M.; Sawaguchi, T.; Matsue, T.; Uchida, I. *J. Phys. Chem.* **1991**, *95*, 9042. (b) Nishizawa, M.; Matsue, T.; Uchida, I. *Anal. Chem.* **1992**, *64*, 2642. (c) Nishizawa, M.; Miwa, Y.; Matsue, T.; Uchida, I. *J. Electrochem. Soc.* **1993**, *140*, 1650. (d) Nishizawa, M.; Matsue, T.; Uchida, I. *J. Electroanal. Chem.* **1994**, *79*, 233.

(11) Nishizawa, M.; Uchida, I. *Electrochim. Acta* **1999**, *44*, 3629.

(12) (a) Shibuya, M.; Nishina, T.; Matsue, T.; Uchida, I. *J. Electrochem. Soc.* **1996**, *143*, 3157. (b) Nishizawa, M.; Yamamura, S.; Itoh, T.; Uchida, I. *Chem. Commun.* **1998**, 1631.

(13) (a) Nishizawa, M.; Koshika, H.; Uchida, I. *J. Phys. Chem. B* **1999**, *103*, 192. (b) Nishizawa, M.; Koshika, H.; Hashitani, R.; Itoh, T.; Abe, T.; Uchida, I. *J. Phys. Chem. B* **1999**, *103*, 4933. (c) Nishizawa, M.; Koshika, H.; Itoh, T.; Mohamedi, M.; Abe, T.; Uchida, I. *Electrochem. Commun.* **1999**, *1*, 375.

(14) Chen, C.; Kelder, E. M.; Jak, M. J. G.; Schoonman, J. *Solid State Ionics* **1996**, *86*, 1301.

(15) (a) Nishizawa, M.; Uchiyama, T.; Dokko, K.; Yamada, K.; Matsue, T.; Uchida, I. *Bull. Chem. Soc. Jpn.* **1998**, *71*, 2011. (b) Nishizawa, M.; Uchiyama, T.; Itoh, T.; Abe, T.; Uchida, I. *Langmuir* **1999**, *15*, 4949.

(16) Guohua, L.; Ikuta, H.; Uchida, T.; Wakihara, M. *J. Electrochem. Soc.* **1996**, *143*, 178.

(17) Dahn, J. R.; Zheng, T.; Thomas, C. L. *J. Electrochem. Soc.* **1998**, *145*, 851.

(18) Robertson, A. D.; Lu, S. H.; Howard, W. F., Jr. *J. Electrochem. Soc.* **1997**, *144*, 3505.

10.1021/cm990696z CCC: $19.00

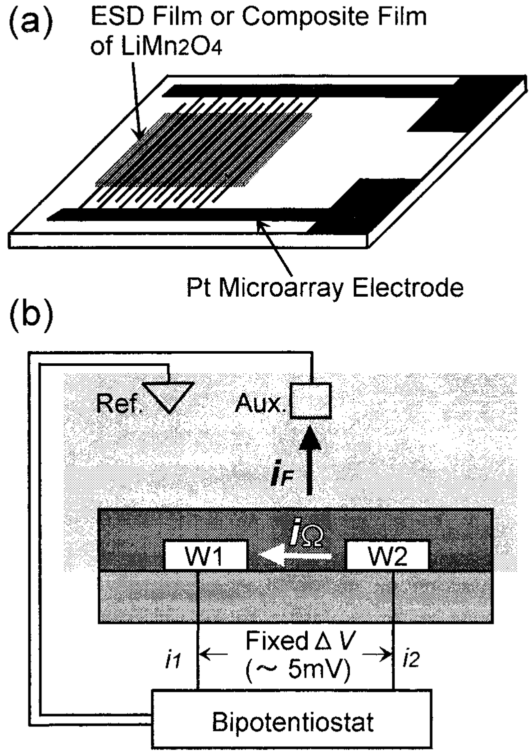

Figure 1. Schematic illustrations of (a) an interdigitated Pt microarray electrode coated with a ESD film or composite film of $LiMn_2O_4$ and (b) the principle of the in-situ conductivity measurement.

mally oxidized silicon wafer, as to have two sets of comb-type Pt arrays; each array has 50 band-electrode elements of 10 μm wide, 2.4 mm long, and 0.1 μm thick, separated by 10 μm from adjacent elements.[11]

The ESD setup used here and working principles were as described previously.[15] Briefly, 12 kV dc voltage was applied between an electrically conductive substrate (IDA electrode) and a stainless steel nozzle (inner diameter, 0.8 mm), which was placed 2 cm above the substrate. An ethanol precursor solution of 25 mM $LiNO_3$ + 50 mM $Mn(NO_3)_2$ was pumped at 2 mL h^{-1} to the nozzle, and the generated spray was transported toward the substrate by electrostatic forces. Since the temperature of the substrate surface was kept at 400 °C during the deposition, owing to the pyrolysis of precursors, a thin layer of $LiMn_2O_4$ was formed as to cover the array electrodes. The films of $LiMn_{1.95}M_{0.05}O_4$ (M: Cr or Co) were prepared by the same procedure except for the composition of the precursor solution. The typical deposition time was 20 min, giving a film thickness of ~0.7 μm. The film morphology was studied using a scanning electron microscope (JSM-5310LV), while the crystalographic structure was studied by X-ray diffraction using Cu Kα radiation with an incident angle of 2° (Shimazu XD-D1).

A commercial $LiMn_2O_4$ particle (Nikki Chemical Co.) was also evaluated as a reference material. The $LiMn_2O_4$ particle of 0.5 g was mixed with 5.5 wt % PVDF and 1.0 wt % acetylene black (DENKA Co.) by using 0.3 mL of *n*-methylpyrolidone (NMP) as a solvent to form a slurry. The resulting viscous slurry was spread on the IDA electrode by means of a doctor blade technique (Yoshimitsu Seiki YBA-1) as to give a film thickness of ~20 μm, followed by drying under vacuum at 130 °C for 12 h. The obtained film is denoted in this paper as a "composite film".

The in-situ conductance measurements were carried out for ESD films and for composite films with a bipotentiostat. As illustrated in Figure 1, the potential of the couple of array electrodes was scanned while maintaining a slight potential bias, ΔV. The values of ohmic (i_Ω) and faradaic current (i_F) can be extracted from the total currents at each electrodes (i_1 and i_2) by data treatment as will be explained later. In this way, we obtain both cyclic voltammograms and conductivity–potential profiles simultaneously. The ionic conductivity of an electrolyte solution is negligible in this dc method. Note, however, that the measurement is a two-point probe method and that the ESD film is polycrystalline, therefore an absolute value for the conductivity cannot be given. Rather, this method is suited to the study of dynamic, relative changes in the conductivity taking place with redox reactions. All electrochemical measurements were conducted by using 1 M $LiClO_4$/propylene carbonate (PC) solutions in a glovebox (Miwa MDB-1B + MS-P15S) filled with dried Ar. The water content of the PC solution (Li ion battery grade, Mitsubishi Kagaku Co.) was less than 20 ppm. Li foils were used as reference and counter electrodes. All electrochemical experiments were conducted at room temperature (~25 °C).

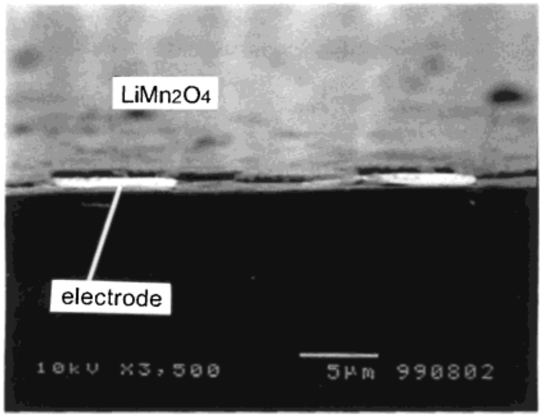

Figure 2. SEM image showing section of $LiMn_2O_4$ ESD film prepared on an IDA electrode substrate.

Results and Discussion

Figure 2 depicts a typical cross-sectional SEM image of a $LiMn_2O_4$ ESD film prepared on an IDA electrode. The film seems to be dense and uniform, which is required for quantitative analysis of the in-situ conductivity. The simultaneous pyrolysis at 400 °C, which is characteristic of the ESD method, is advantageous to eliminate the effect of gas evolution during decomposition on the morphology of resulting films.[15] All the XRD peaks of the ESD film were assigned to $LiMn_2O_4$, justifying spinel formation without any other phases.

Figure 3a shows typical current responses obtained with the IDA electrodes (W1 and W2) coated with a $LiMn_2O_4$ ESD film. These data contain both faradaic current (i_F) due to the lithium insertion/extraction reaction and ohmic current (i_Ω) flowing between the array through the film. If we assume that the magnitudes of i_F are equal at both electrodes because of the small ΔV (5 mV), the values of i_Ω and i_F can be extracted from the total currents by

$$i_\Omega = (i_2 - i_1)/2 \tag{1}$$

$$i_F = (i_2 + i_1)/2 \tag{2}$$

and thus the conductivity of the film is calculated as follows:

$$\sigma = i_\Omega w / nld\Delta V (\mathrm{S\ cm^{-1}}) \tag{3}$$

where w is the gap width of arrays (10 μm); n (= 50), the total number of the band electrodes; l, the length of

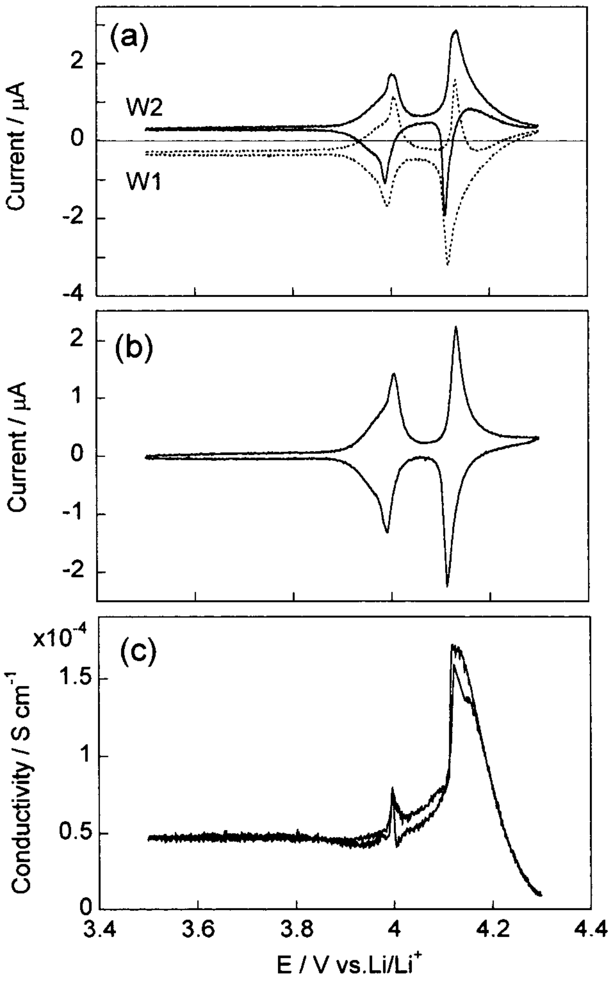

Figure 3. (a) Current responses of $LiMn_2O_4$ ESD film on IDA electrode upon a potential cycling at the scan rate of 0.2 mV s^{-1} with keeping 5 mV potential difference between W1 and W2. Cyclic voltammogram (b) and potential−conductivity profile (c) were derived by using eqs 2 and 3, respectively.

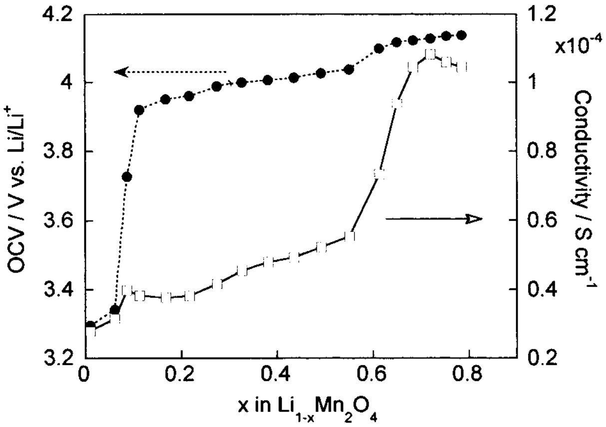

Figure 4. The variations of open-circuit voltage (circle) and conductivity (square) of $Li_{1-x}Mn_2O_4$ as a function of *x*.

an electrode element (2.4 mm); and *d*, the thickness of the film (0.7 μm). Figure 3b shows the cyclic voltammogram (i_F profile) derived in this way. Two couples of oxidation and reduction peaks appeared clearly at ∼4.0 and 4.15 V vs Li/Li^+, being accompanied by extraction/insertion of lithium ion from/into the manganese spinel phase.[1−9] Figure 3c depicts the conductivity−potential profile obtained by eq 3. The shape of conductivity profile did not depend on the direction of potential scan. The measured conductivity was in the range of 10^{-4} S cm^{-1}, being roughly in agreement with previous reports.[8,19−21] The conductivity data exhibited a pronounced peak-shape profile having a maximum at around 4.15 V. Such a transient increase in the conductivity during the course of lithium extraction (and reinsertion) in $Li_{1-x}Mn_2O_4$ is unexpected and reported here for the first time. The magnitudes of i_F at two working electrodes are not strictly the same in practice. Such deviation will be interpreted as a change of conductivity by our data analysis. For example, a spiky and small increase in conductivity at 4.0 V seems to be caused by the slight difference in magnitudes of i_F at two working electrodes. We denote herein this kind of error in conductivity profile as “faradaic noise”.

To confirm potentiodynamic results in Figure 3, we also conducted a measurement under open-circuit conditions. A known amount of charge was induced, and then the open-circuit voltage (OCV) and conductivities of the $Li_{1-x}Mn_2O_4$ films were measured after more than 2 h. In this case, we can simply obtain the conductivity values at each OCV without faradaic noise. The conductivity was calculated from the current at 5 mV dc bias voltage applied between the array electrodes using a source measure unit (Keithley 236). The measured current was roughly proportional to the bias voltage (5−50 mV), and was stable for at least 30 min. These facts indicate that the ion transport of Li^+ through the electrolyte solution [22] can be ruled out from conduction path, at least for our measurement condition. Figure 4 presents the plots of OCV and conductivity as a function of *x*. Two potential plateaus were observed around 4.0 and 4.15 V in the OCV curve, corresponding to the CV peaks. The variation of conductivity against *x* was essentially the same as the observation in Figure 3c. The conductivity of the film tends to increase with decreasing the lithium content in the spinel, and the increasing behavior is pronounced for the reaction taking place at 4.15 V rather than the reaction at 4.0 V. Unfortunately, since the OCV corresponding to $x >$ 0.8 was unstable probably due to self-discharge coupled with a oxidative decomposition of electrolyte solution, we cannot represent the conductivity decrease for the fully delithiated manganese spinel (λ-MnO_2).

$Li_{1-x}Mn_2O_4$ spinel is a mixed-valence (Mn^{3+}/Mn^{4+}) compound and its electronic conduction takes place by electron-hopping between high-valence (Mn^{4+}) and low-valence (Mn^{3+}) cations.[8] Conductivity of this type would be governed by (i) the amount of carrier (electron of Mn^{3+}) and (ii) the hopping length (Mn−Mn interatomic distance). The amount of electron carrier decreases proportionally with the degree of delithiation coupled with oxidation of Mn^{3+} to Mn^{4+}. On the other hand, the Mn−Mn distance in the spinel structure is contracted by delithiation. The measured conductivity change may result from the sum of these opposite effects. The

---

(19) Kanoh, H.; Feng, Q.; Hirotsu, T.; Ooi, K. *J. Electrochem. Soc.* **1996**, *143*, 2610.

(20) Schutte, L. Colsmann, G.; Reuter, B. *J. Solid State Chem.* **1979**, *27*, 227.

(21) Molenda, J.; Swierczek, K.; Kucza, W.; Marzec, J.; Stoklosa, A. *Solid State Ionics* **1999**, *123*, 155.

(22) Baudais, M. E. F.; Dahn, J. R. *Solid State Ionics* **1993**, 66, 175.

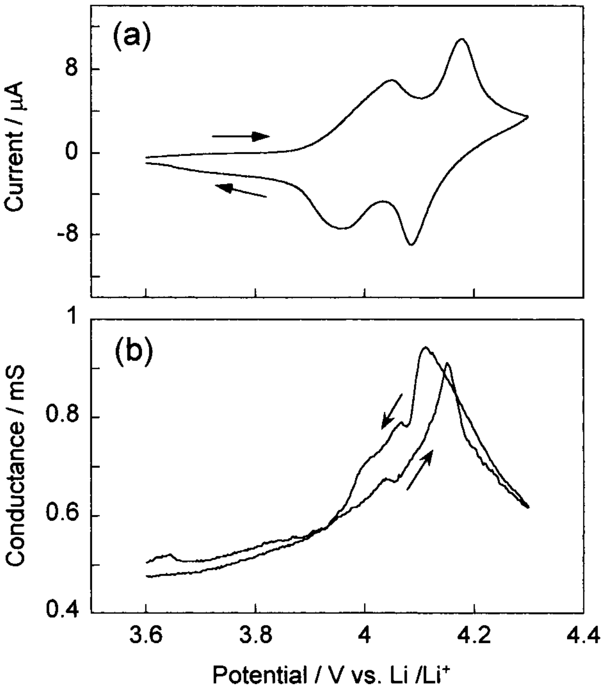

Figure 5. Cyclic voltammogram (a) and conductance–potential profile (b) of a composite film of commercialized $LiMn_2O_4$ powder, taken at 0.02 mV s^{-1} with 5 mV potential bias.

conductivity of $Li_{1-x}Mn_2O_4$ increases transiently during the delithiation process, indicating that the effect of contraction of hopping length was more predominant than the decrease of the amount of the electron carrier. Importantly, the conductivity increase was pronounced especially for the reaction at 4.15 V. The lithium insertion/extraction reaction of $Li_{1-x}Mn_2O_4$ in this potential region (average $x \geq 0.5$) has been categorized as a two-phase process, in which two cubic phases (a_c = 8.045 Å and 8.142 Å) coexistent without any intermediate lattice constant.[6] Therefore, during the course of delithiation, $Li_{0.5}Mn_2O_4$ would change partly to λ-MnO_2 according to the degree of lithium extraction. To explain the apparent high conductivity observed around 4.15 V, it may be possible to speculate that the most contracted λ-MnO_2 phase can act as an effective "conduction path" for the electron carrier originating in $Li_{0.5}Mn_2O_4$. As seen in Figure 3c, the fully delithiated spinel (λ-MnO_2 as a whole) showed lower conductivity because of exhaustion of electron carrier.

In additional experiments, we carried out in situ conductance measurement for a composite film of commercialized $LiMn_2O_4$ powder using the IDA system. The procedure for film preparation was described in the Experimental Section. Figure 5 shows the resulting voltammogram and the conductance–potential profile. The obtained profiles were relatively vague and unstable due to complications of interparticle connections within composites.[13c] Since the transient increase in the conductance was also observed for the commercialized $LiMn_2O_4$ powder, results shown in Figures 3 and 4 are not specific to the ESD film prepared at low temperature (400 °C), rather it is general chemistry of $Li_{1-x}Mn_2O_4$. It should be mentioned that we reported previously that the "sputter-deposited" $LiMn_2O_4$ film showed no significant conductivity change during its lithium insertion/extraction reaction.[23] The composition of the sputtered film may slightly deviate from $LiMn_2O_4$ due to differences in sputtering rates between elements.

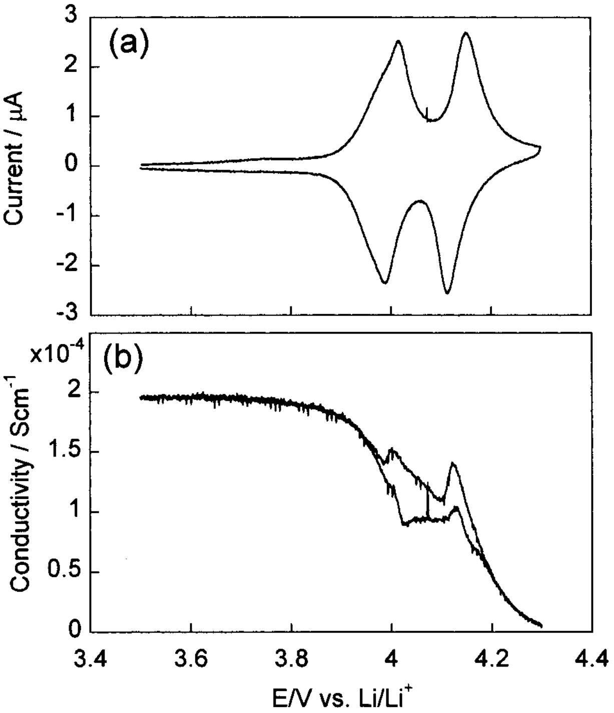

Figure 6. Cyclic voltammogram (a) and conductivity–potential profile (b) of a $LiMn_{1.95}Cr_{0.05}O_4$ ESD film, taken at 0.2 mV s^{-1} with 5 mV potential bias.

Figure 6 shows the voltammogram and the conductance–potential profile for the $LiMn_{1.95}Cr_{0.05}O_4$ film prepared by ESD methods. The partial substitution of manganese with other metal cation such as Cr^{3+} was reported to improve the stability of spinels against Jahn–Teller distortions and/or the dissolution of manganese into electrolytes.[16–18] While the CV shape broadened to some extent, the essential voltammetric feature was the same as that of unsubstituted spinel; two couples of oxidation and reduction peaks appeared around 4.0 and 4.15 V vs Li/Li^+. Initial conductivity at the composition of $LiMn_{1.95}Cr_{0.05}O_4$ was found to be 4 times larger than that of $LiMn_2O_4$. The cubic lattice constant is decreased by the manganese substitution,[16,17] probably being responsible for the observed higher conductivity with shorter hopping length. During the delithiation reaction, the conductivity started to decrease at 3.9 V. Although some faradaic noise is superposed, the conductivity seems to decrease continuously until the spinel is fully delithiated. We confirmed this feature by open-circuit conductivity measurements (not shown). It was reported with XRD analysis[16] that the two-phase region disappeared after Cr^{3+}-doping. Therefore, the results obtained here for $Li_{1-x}Mn_{1.95}Cr_{0.05}O_4$ may support our speculation that the transient conductivity increase for $Li_{1-x}Mn_2O_4$ may result from phase transformation. We also studied the in-situ conductivity of $LiMn_{1.95}Co_{0.05}O_4$ ESD films. The Co^{3+}-doped spinel showed a monotonic decrease in its conductivity–potential profile, as was observed for Cr^{3+}-doping. Further work is on going to clarify the effect of doping content as well as the kind of admetals.

---

(23) Yamamura, S.; Koshika, H.; Nishizawa, M.; Matsue, T.; Uchida, I. *J. Solid State Electrochem.* **1998**, *2*, 211.

Conclusion

By means of an IDA electrode with a bipotentiostat, we evaluated both cyclic voltammograms and potential–conductivity profiles of $Li_{1-x}Mn_2O_4$ thin film, simultaneously. A peak-shaped transient conductivity increase was observed for the first time. Although further work is needed to clarify details, the two-phase reaction mode seems to be responsible for the observed conductivity profile.

We studied mainly the conductivity of active material itself without any additives such as polymer binders. From a practical standpoint, however, the total conductance of composite films may be rather important. Electrical conductance of the composite films originates from electrical interparticle connections within the composite as well as the conductivity of the active material itself. Our technique using IDA electrodes is also a powerful tool to optimize preparation of high performance composite electrodes with high retention of conductance during charge/discharge of batteries.[13c]

Acknowledgment. The present work was supported by Grant-in-Aids for Encouragement of Young Scientists (No. 09750906), for Scientific Research on Priority Area (No. 10148205 for “New Protium Function”) and for Scientific Research (B) (No. 10555297) from the Ministry of Education, Science, Sports and Culture, Japan.

CM990696Z